Biophys Rev
DOI 10.1007/s12551-017-0298-y

REVIEW

The many faces (and phases) of ceramide and sphingomyelin II – binary mixtures

María Laura Fanani[1] · **Bruno Maggio**[1]

Received: 28 May 2017 / Accepted: 27 July 2017

Abstract A rather widespread idea on the functional importance of sphingolipids in cell membranes refers to the occurrence of ordered domains enriched in sphingomyelin and ceramide that are largely assumed to exist irrespective of the type of N-acyl chain in the sphingolipid. Ceramides and sphingomyelins are the simplest kind of two-chained sphingolipids and show a variety of species, depending on the fatty acyl chain length, hydroxylation, and unsaturation. Abundant evidences have shown that variations of the N-acyl chain length in ceramides and sphingomyelins markedly affect their phase state, interfacial elasticity, surface topography, electrostatics, and miscibility, and that even the usually conceived "condensed" sphingolipids and many of their mixtures may exhibit liquid-like expanded states. Their lateral miscibility properties are subtlety regulated by those chemical differences. Even between ceramides with different acyl chain length, their partial miscibility is responsible for a rich two-dimensional structural variety that impacts on the membrane properties at the mesoscale level. In this review, we will discuss the miscibility properties of ceramide, sphingomyelin, and glycosphingolipids that differ in their N-acyl or oligosaccharide chains. This work is a second part that accompanies a previous overview of the properties of membranes formed by pure ceramides or sphingomyelins, which is also included in this Special Issue.

Keywords Surface miscibility · Langmuir films · Compression isotherms · Phase diagrams · Brewster angle microscopy

Introduction

The concept of "miscibility" can be quite ambiguous and misleading if not clearly focused on the particular scale range to which it is applied (Maggio 2004). For example, at the local nm level, molecular immiscibility (or ideal full miscibility) in binary monolayers (with or without macroscopic phase domain separation on the μm scale range) can be inferred by the existence of smooth surface pressure–area isotherms, linear additive variation of mean molecular area, and dipole potential density as a function of the film composition, together with composition-invariant collapse pressures (Phillips 1972; Brockman 1994; Maggio et al. 1997; Carrer and Maggio 2001; Maggio 2004). In binary or ternary systems, lateral immiscibility can be visually observed on the μm scale range by the presence of segregated phase or compositional domains (McConnell 1990; Möhwald 1995; Oliveira and Maggio 2000, 2002; Fanani et al. 2002; Rosetti et al. 2003). However, when the system is rather complex regarding composition or surface topography, the emergence of lateral thermodynamic tensions and interfacial energy terms blurs away and impairs the detection of molecular cooperativity at the local level. This has the consequence of the film showing smooth compression isotherms, lacking the usual pressure-induced two-dimensional transitions or partial film collapse of immiscible segregated phase states; this could likely be erroneously interpreted as a homogeneously mixed surface while it may actually exhibit a

This article is part of a Special Issue on 'Latin America' edited by Pietro Ciancaglini and Rosangela Itri.

✉ María Laura Fanani
lfanani@fcq.unc.edu.ar

[1] Centro de Investigaciones en Química Biológica de Córdoba (CIQUIBIC-CONICET), Departamento de Química Biológica Ranwell Caputto, Facultad de Ciencias Químicas, Universidad Nacional de Córdoba, Haya de la Torre y Medina Allende, Ciudad Universitaria, X5000HUA Córdoba, Argentina

Published online: 19 August 2017

richly featured surface topography on the mesoscopic level, with coexistence of immiscible domains of different composition and phase state (Oliveira and Maggio 2000, 2002; Fanani et al. 2002; Rosetti et al. 2003, 2005). On the other hand, the existence of microheterogeneity on the μm scale range in the surface topography implies the existence of local interactions leading to unfavorable intermolecular mixing of at least some of the components along the lateral plane. For example, monolayers with quite a complex lipid–protein composition (prepared with the whole myelin membrane) exhibit smooth compression isotherms but labeling of ganglioside GM1, GalCer, and other components localize in segregated surface domains (Oliveira and Maggio 2002).

Early conclusions on the basis of calorimetric and monolayer studies (Maggio et al. 1978b) indicated unfavorable self-interactions among sphingolipids, but favorable mixing with glycerophospholipids (Maggio 2004; Maggio et al. 2004). Also, the assumption that direct interactions among carbohydrates in the polar head groups of glycosphingolipids (GSLs) could cause self-association has received no supportive experimental evidence. On the contrary, it was shown that the presence of a lactose moiety in the polar head group works against homo-association and actually weakens intermolecular interactions by reducing packing efficiency by contributing to "bulkiness" but not "stickiness" (Regen 2002); this was indicated many years ago by the progressive increase of the GSLs mean molecular area and decrease of their Tm as their oligosaccharide chains become more complex (Maggio et al. 1978a, 1985). It is necessary to emphasize that the point is not if some type of sphingolipid can be found in segregated enriched domains (an established fact) or if topographical domains occur in biomembranes (surface microheterogeneity is also well proven), but what is the *initial driving potential* at the local molecular level for spontaneous sphingolipid segregation in domains and how thermodynamically stable or long-lived such associations might be in the dynamic interfacial conditions (let alone introducing further harsh conditions for their putative isolation). So far, the reason for sphingolipid enrichment in segregated domains does not appear to be accounted for only by their individual molecular properties or chemical structure, such as the hydrogen bonding capacity of the amide linkage.

The presence of sphingolipids has been considered a major factor for detergent solubility of putatively condensed membrane domains. However, sphingolipids by themselves (and specially GSLs) do not hinder but generally increase propensity to solubilization (Sot et al. 2002); the higher the sphingomyelin (SM) proportion in systems with phosphatidylcholine, the less detergent required for its solubilization (Hertz and Barenholz 1975; Sot et al. 2002). Thus, the condensed or expanded behavior, gel phase states, or liquid-ordered phases per se do not imply detergent insolubility. For natural PCs (T_ms in the range of − 10 to 65 °C) and for pure SM (T_m ~ 40 °C), the gel phase state actually requires less detergent for solubilization, compared to the liquid-crystalline phase (Patra et al. 1998, 1999). IR and EPR of PC/SM and PC/SM/cholesterol showed H-bonding between amide carbonyl of SM and hydroxyl of cholesterol, but the sterol contributes more to detergent insolubility at 37 °C than at 4 °C. PC weakens the interactions between SM and cholesterol in the liquid-ordered phase and facilitates detergent solubility (Veiga et al. 2000; Pilar Veiga et al. 2001) and the mixtures are detergent-solubilized at least equally, but generally more easily at 4 °C than at 37 °C. The detergent itself induces lipid redistribution and formation of insoluble associations (Heerklotz 2008).

The following boxes summarize findings from the references quoted in the paragraph above.

Cross-linking monomers	Heterodimer, homodimer
PC14/PC14	1.01
PC14/PC18	1.67
SM18(14)/PC18(PC14)	2.02
CerLac18(14)/PC18(PC14)	1.77

Results are similar in LO mixtures containing 29 mol% cholesterol

Detergent solubility of selected mixtures

		D_{50} (mM)
PC/SM/Ch (3:1:1)		
[4 °C]	More soluble	2.8
[37 °C]	Less soluble	>>5
PC/Cb/GM3/Ch (6:1:1:2)		
[4 °C]	More soluble	1.3
[37 °C]	Less soluble	2.7
PC/SM/Cb/Ch (6:1:1:2)		
[4 °C]	More soluble	3.2
[37 °C]	Less soluble	4.1
PC/SM/GM3/Ch (6:1:1:2)		
[4 °C]	More soluble	1.8
[37 °C]	Less soluble	1.9
PC/Cb/GM3/Ch (2:1:1:2)		
[4 °C]	More soluble	2.7
[37 °C]	Less soluble	3.3

The interaction of some species of SM and ceramide (Cer) has been studied in monolayers (Busto et al. 2009) and bilayers (Busto et al. 2009; Westerlund et al. 2010). 16:0 Cer forms condensed domains segregated from more liquid-like phases enriched in SM (Busto et al. 2009) and unsaturated PCs (Castro et al. 2007; Pinto et al. 2011) even in the presence of low amounts of cholesterol (Silva et al. 2007; Ale et al. 2012), leading to the idea that Cer and cholesterol can compete in ordered domains with SM (Staneva et al. 2008; Busto et al. 2010). Mixtures of Cer and SM N-acylated with palmitic acid

(16:0) in monolayers show a thermodynamically stable point at $X_{16:0\ Cer} = 0.4$ with molecular area condensation, whereas in bilayer systems, complex differential scanning calorimetry (DSC) thermograms occur (Busto et al. 2009) with increasing melting temperatures at increasing ceramide content. A similar behavior was also reported for mixtures of 16:0 SM with 12:0, 18:0, and even 24:1 Cer (Westerlund et al. 2010). On the other hand, the interaction with the shorter N-acyl chain length 4:0 and 8:0 Cers resulted in complex thermograms, but at decreasing temperatures.

Ceramide mixtures

Ceramides are the simplest two-chained sphingolipids and those with long saturated acyl chains exhibit strong intermolecular association. As a consequence, such Cers form segregated solid-like condensed domains, in both bilayers and monolayers, that even exclude fluorescent probes and proteins (Carrer and Maggio 1999; Holopainen et al. 2001; Härtel et al. 2005; Castro et al. 2007; Chiantia et al. 2008; Busto et al. 2009; Karttunen et al. 2009; López-Montero et al. 2010). Natural mixtures of Cer are mainly composed of long chain Cers. In particular, chicken egg Cer has 84% of 16:0 Cer and its surface behavior closely resembles that of pure 16:0 Cer (Fanani and Maggio 2010; Catapano et al. 2015). Lopez-Montero and co-workers described the solid character of natural Cer monolayers by shear surface rheology studies (Catapano et al. 2011, 2015; López-Montero et al. 2013). High compression and shear moduli were measured at room temperature, which constitutes a signature for the solid character. Ceramide monolayers undergo plastic deformations in response to an applied stress exceeding the yield point (López-Montero et al. 2013). This unique feature has converted Cers into the paradigm of rigid lipids. Upon heating, natural Cer film undergoes a solid to fluid transition, which was evidenced as a vanishing shear rigidity at lower temperatures than the lipid melting temperature. Additionally, a process compatible with a glassy behavior was found upon cooling. This behavior was also correlated with calorimetric behavior of egg Cer suspensions (Catapano et al. 2015). This has somehow introduced the unfortunate erroneous bias, especially acknowledged in the cell membrane biology field, that *all* Cers would be condensed type of compounds forming solid-like domains at all degrees of surface density.

However, Cers occur with a variety of N-acyl chain lengths, as mentioned in this revision work in Part I of this Special Issue, and those with chain lengths shorter than the hydrocarbon moiety of sphingosine can form expanded phases and undergo typical monolayer liquid-expanded (LE) to liquid-condensed (LC) phase transitions at room temperature and defined surface pressures (Dupuy et al. 2011). The strong influence of the type of N-linked acyl chain is also reflected in the behavior of 10:0 Cer mixed with Cers of increasing acyl chain length. The mixtures of 10:0–12:0 Cer showed ideal mixing, even though their minimal mismatch in acyl chain length resulted in a considerable difference in the tendency to adopt the condensed state (Dupuy and Maggio 2012). It is worth mentioning that, in the phase transition region of each mixture, the surface topography reveals condensed domain shape evolving from small and rounded 10:0 Cer domains in films with high proportions of this Cer to large flower-like domains similar to those of pure 12:0 Cer in films enriched in the latter lipid (Fig. 1). The population of condensed domains observed during the monolayer phase transition and the narrow range of surface pressure over which domain formation takes place also supports that the behavior of the mixture resembles that of a single molecular entity that cooperatively transforms from an expanded to a condensed state.

At 24 °C, 14:0 Cer is able to form mixed expanded phases with 10:0 Cer. When the content of 14:0 Cer is above 50 mol%, partial de-mixing and coexistence of condensed phases of the components occurs at high surface pressures as observed by BAM: a 14:0 Cer-enriched phase formerly nucleates in domains and a continuous 10:0 Cer-enriched phase undergoes the LE–LC transition at surface pressures close to the transition pressure of pure 10:0 Cer (Dupuy and Maggio 2012). The partial miscibility of 10:0 Cer and 14:0 Cer with formation of a 10:0 Cer- enriched phase explains the non-horizontal phase coexistence region of the surface pressure–molecular area isotherm of the mixtures (Fig. 1).

Delayed domain growth yields a non-zero rigidity at the phase coexistence region during film compression (Arriaga et al. 2010). The resistance to the phase change would be a consequence of a balance of the energy necessary for nucleation of more condensed domains and the line tension and plasticity of the more liquid phase that opposes domain growth in the film where the condensed phase is formed. In the 14:0/10:0 Cer mixture, the presence of the longer N-acyl chain length in the expanded phase increases the rigidity, which should also contribute to the increase of the surface pressure necessary to achieve phase coexistence. Cers with N-linked acyl chains longer than 18 carbons produce condensed films that, different to 14:0 Cer, give rise to phase coexistence when mixed with 10:0 Cer at both low and high surface pressures over the whole range of composition (Fig. 1). The topography of the mixtures visualized by BAM confirmed phase separation at low and high surface pressures. At low surface pressure, 18:0 Cer-enriched condensed domains are surrounded by a 10:0 Cer-enriched expanded phase and show smaller rounded or thinner striped shapes when compared to condensed domains observed in the mixtures of 14:0 Cer/10:0 Cer.

The effect of hydrophobic mismatch is further clarified by comparing the surface behavior of the pairs 14:0 Cer/10:0 Cer

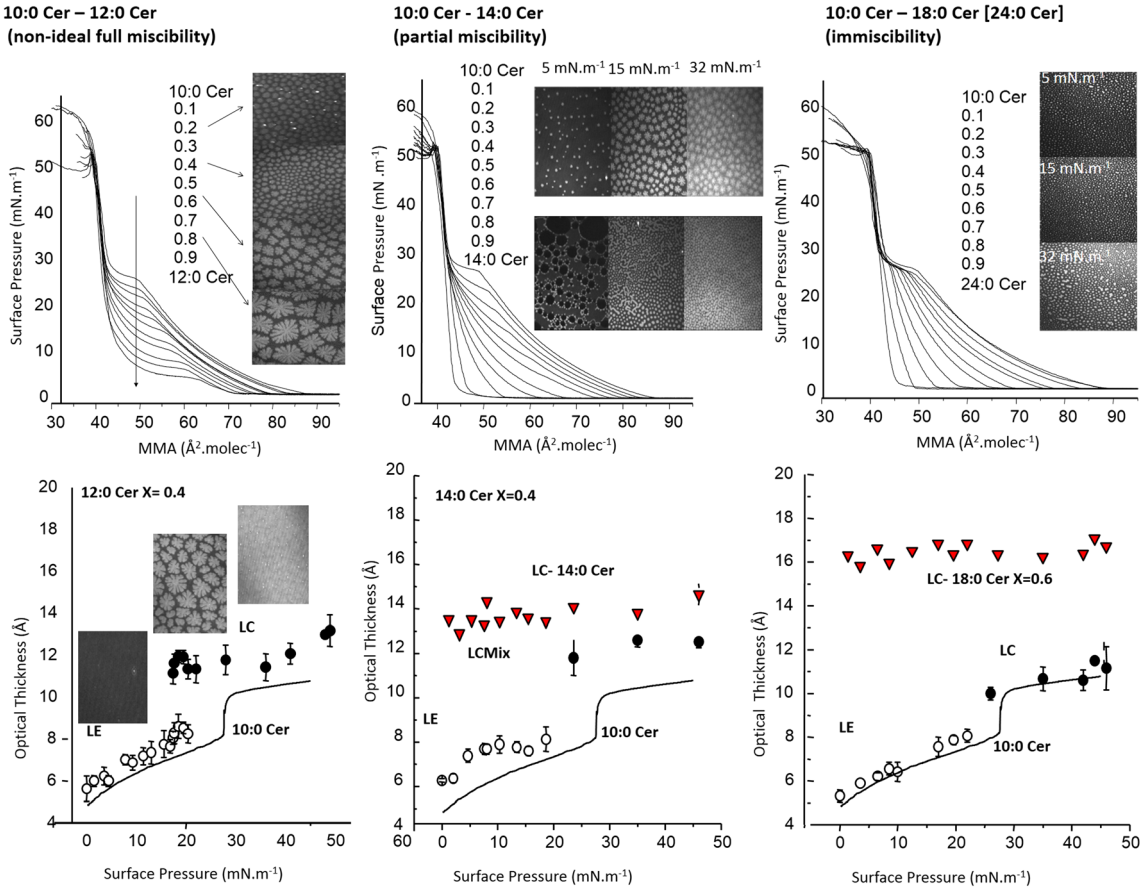

Fig. 1 Surface behavior and topography of mixed monolayers of ceramides. The upper panels show the compression isotherms of the pure and mixed films as indicated. The lower panels show the monolayer thickness calculated from reflectivity measurement as a function of surface pressure. The expanded phase (*open circles*) thickens at increasing values of surface pressure up to the transition surface pressure, when domains of condensed phase appear (*solid symbols*). The insets show representative Brewster angle microscopy images of the corresponding films. All images are 200 × 250 μm in size. Adapted from Dupuy and Maggio (2012)

at 23 °C and 16:0/12:0 Cer at 40 °C. Both systems possess the same hydrocarbon chain length difference between the sphingoid and N-acyl chains, but enhanced van der Waals interactions would be expected for the mixture containing longer acyl chains, such as 16:0/12:0 Cer. On the contrary, the mixtures displayed very similar behavior when force–area curves were compared, showing similar dependence (decrease) of the transition surface pressure with variations of the film composition, indicative of the mixing of Cers in the expanded state. Thus, N-acyl chain length determines both the phase behavior and the mixing in Cer monolayers (Dupuy and Maggio 2012).

In phospholipid bilayers, the hydrophobic mismatch between the components in binary mixtures leads to different types of phase diagrams (Mabrey and Sturtevant 1976; de Almeida et al. 2005). For PCs, a difference of six carbons in the acyl chain length in the mixture of symmetric dilauroyl-PC/distearoyl-PC produced a rather flattened fluid–gel coexistence line (Mabrey and Sturtevant 1976; Risbo et al. 1995). In monolayers of asymmetric Cers N-acylated with saturated fatty acids, a difference of eight carbons in the N-acyl chain length mismatch was necessary to yield a similar mixing behavior of a solid/gel phase in equilibrium with an LE/liquid crystalline one. On the other hand, both in symmetric PC bilayers and in monolayers of asymmetric Cers, a hydrophobic mismatch of only two carbons (dimiristoyl-PC/dipalmitoyl-PC and 12:0 Cer/10:0 Cer) produced mixtures with almost ideal mixing behavior (Mabrey and Sturtevant 1976). A correlation of the mixing behavior in bilayers and monolayers was also observed for a hydrophobic mismatch of four carbons in both systems: an LE phase composed of both components in the mixture and a condensed phase coexisting with the LE phase over a broad range of temperatures and surface pressures (for the bilayers or monolayers, respectively) (Dupuy and Maggio 2012).

Under conditions in which homogeneous expanded films of mixtures of a long and a short chain Cer (14:0/10:0 Cer; 16:0/12:0 Cer) are formed, there are no differences in the surface compressibility moduli compared to the LE phase of the pure short chain Cer. Actually, at 15 $mN.m^{-1}$, the C_S^{-1} remain invariant with composition at $X_{14:0Cer} < 0.5$, indicating that the elasticity of the whole film in this composition range is

accounted for by the continuous expanded phase. On the other hand, BAM imaging shows that the LE phase of the film is homogeneous at the micrometric level and shows a *p*-reflectivity higher than that of 10:0 Cer at comparable surface pressures (Dupuy and Maggio 2012). The latter results point indicate that the expanded state is actually composed by 10:0 Cer and the thicker 14:0 Cer. At $X_{14:0\ Cer}$ above 0.5, the excess of the long chain Cer and the condensed domains leads to an increase of the surface compressional modulus and, consequently, to increased amounts of condensed phase in the mixture. In this manner, the elastic properties of the film do not change under the incorporation of a more solid state-prone lipid such as 14:0 Cer and, as long as the LE phase is able to accommodate the molecules, no phase separation occurs. The condensed domains in equilibrium with the expanded phase impose dynamic rigidity or stiffening upon compression but retain a global state typical of expanded phases (Wilke and Maggio 2009; Wilke et al. 2010). In this manner, the increased amount of domains in the 18:0/10:0 Cer as compared to the 14:0/10:0 Cer mixture can also explain the higher values of the compressibility modulus by imposing more resistance to compression.

Mixtures of ceramides with sphingomyelins and glycerophospholipids

The interaction of some species of SM and Cer was studied in monolayers (Busto et al. 2009; Wilke and Maggio 2009) and bilayers (Busto et al. 2009; Westerlund et al. 2010), as well as natural mixtures of Cer and SM (Catapano et al. 2011). 16:0 Cer forms condensed domains segregated from fluid phases enriched in 16:0 SM (Busto et al. 2009) and unsaturated PCs (Castro et al. 2007; Pinto et al. 2011) even in the presence of low amounts of cholesterol (Silva et al. 2007), leading to the idea that Cer and cholesterol can compete in ordered domains with SM (Staneva et al. 2008; Busto et al. 2010). Mixtures of Cers and SMs N-acylated with palmitic acid (16:0) at the air−water interface showed a thermodynamically stable point at $X_{16:0\ Cer} = 0.4$ with molecular area condensation, whereas in bilayer systems, complex DSC thermograms were reported (Busto et al. 2009) with increasing melting temperatures at increasing 16:0 Cer content. A similar behavior was also reported for mixtures of 16:0 SM with 12:0, 18:0, and even 24:1 Cers (Westerlund et al. 2010). On the other hand, the interaction with the shorter N-acyl chain length 4:0 and 8:0 Cers resulted in complex thermograms but at decreasing temperatures. By means of nuclear magnetic resonance, Leung et al. (2012) measured the specific melting of 16:0 SM and 16:0 Cer upon gel-to-liquid crystalline phase transition using perdeuterated palmitic acid N-acylated in either Cer or SM; it was demonstrated that Cer induced gel-phase stabilization by hydrocarbon chain ordering upon mixing and melting of the SM component at slightly lower temperatures.

At low surface pressures, the mechanical properties of 16:0 Cer and 16:0 SM mixtures are related to the crowding effect of Cer-enriched domains immersed in an SM-enriched continuous phase in the LE state. The monolayer viscosity depends on the lateral pressure and on the domain–domain distance. The viscosity change with pressure is caused by both an increase of intrinsic viscosity and an increase in domain crowding, whilst as the domain array is relaxed, repulsive dipolar interactions appear to acquire importance (Wilke and Maggio 2009). At high surface pressures (> 20 mN/m), the films composed of a natural mixture of SM (egg SM) are present as disordered solid or LC state with a rheological response typical of a fluid system. On the other, hand egg Cer show a finite shear response, typical of a solid state, as has been commented above (López-Montero et al. 2010), with higher elastic storage than viscous losses. Egg Cer increases the solid character of SM-based membranes and decreases their fluidity, thus drastically decreasing the lateral mobilities of embedded objects (Catapano et al. 2011). The mixed film containing egg Cer/egg SM (1:2) showed an intermediate viscous character, a fact that can be related to the 1:2 maximal compaction due to the molecular complexation previously hypothesized by Busto et al. (2009).

The physical properties of Cer interaction with glycerophospholipids in model membranes revealed important effects on membrane permeability (Ruiz-Argüello et al. 1996; Siskind and Colombini 2000), transbilayer flip-flop lipid motion (Contreras et al. 2003), and lateral domain segregation (Huang et al. 1996; Carrer and Maggio 1999; Veiga et al. 1999). Cer-induced domain segregation in several lipid mixtures with glycerophospholipids (Huang et al. 1996; Carrer and Maggio 1999; Veiga et al. 1999; Fanani et al. 2002; Hsueh et al. 2002; Sot et al. 2005, 2006; Carrer et al. 2006) has been reported using different biophysical approaches [see Goñi and Alonso (2006, 2009) for reviews]. Cers induce high-temperature melting domains in mixtures where phospholipids display low (palmitoyl-oleoyl-PC) (Hsueh et al. 2002) and high (dipalmitoyl-PC or dielaidoyl-phosphatidylethanolamine) (Carrer and Maggio 1999; Sot et al. 2005) gel-to-fluid phase transition temperatures. A microscopy study combining DSC, fluorescence spectroscopy, and confocal fluorescence on the interaction of egg Cer with its relative egg SM showed the segregation of detergent-resistant Cer-enriched domains (Sot et al. 2006). In either premixed or enzyme-generated systems with bovine brain SM [mainly stearic (18:0) and lignoceric (24:0) acyl chains], Cer induces morphologically different Cer-enriched domains, depending on how the mixture was generated (Fanani et al. 2002, 2009; De Tullio et al. 2008). Furthermore, different types of Cer-enriched domains are enzymatically formed in the presence of cholesterol, showing high solubility in cholesterol-rich membranes (Silva et al. 2009; Ale et al. 2012).

Saturated acyl chains are associated with stronger interactions with the glycerophospholipid and with generation of condensed lipid domains. Differences in acyl chain length induce membrane interdigitation (Carrer et al. 2006; Pinto et al. 2008) and are the cause of some cases of phase separation. However, similar results based on DSC of vesicles containing natural Cers of different length do not support a similar assumption (Veiga et al. 1999). Monolayer and bilayer approaches were employed to study the mixture of 16:0 SM/16:0 Cer. In both systems, 16:0 Cer exerts a number of effects in a composition-dependent manner up to $X_{16:0\ Cer}$ 0.3–0.4 (Busto et al. 2009). An interpretation of the data on the basis of lipid bilayer observations (Sot et al. 2006) is that 16:0 Cer-rich and 16:0 Cer-poor phases are immiscible and phase-segregated. In the range $X_{16:0\ Cer}$ 0–0.4, monolayer experiments show a strong condensing effect exerted by the addition of 16:0 Cer (Fig. 2). This appears to be due to the incorporation of 16:0 SM into 16:0 Cer-enriched LC domains with a concomitant phase state change of the 16:0 SM molecules from LE to LC (Fig. 2). The estimation of two coexisting phases in 16:0 SM-rich monolayers, composed of ~5 and 30 mol% 16:0 Cer, respectively, is compatible with the measurements performed in vesicle bilayers. In the limit case of 30 mol% 16:0 Cer, a 16:0 SM-rich DSC endotherm is no longer visible in mixtures containing >30 mol% 16:0Cer, and GUVs containing >40 mol% 16:0 Cer cannot be formed (Busto et al. 2009), presumably because a certain proportion of the 16:0 SM-rich bilayer is required for vesicle stability. Several independent observations suggest the existence of more than one 16:0 Cer-enriched phase. The LC (16:0 Cer-enriched) phase observed in monolayers at $X_{16:0Cer} > 0.4$ is, in fact, a mixture of two condensed phases (Busto et al. 2009). Also, Sot et al. (2006) observed domain coexistence over a large region of the egg SM/egg Cer temperature-composition diagram by using calorimetric, fluorescence quenching, and temperature-dependent turbidimetric measurements.

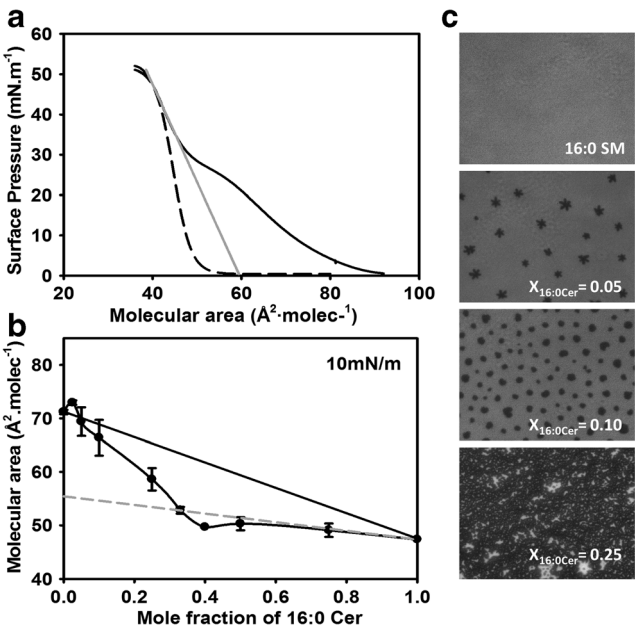

Fig. 2 Condensation of 16:0 SM induced by the presence of 16:0 Cer. (**a**) Compression isotherms of pure 16:0 SM (*solid line*) and pure 16:0 Cer (*dashed line*) and the extrapolated molecular area for 16:0 SM in a condensed phase at low surface pressures (*straight gray line*). (**b**) Variation of the mean molecular area of the 16:0 SM–16:0 Cer mixture with 16:0 Cer mole fractions at 10 $mN.m^{-1}$. The *solid line* represents the molecular area for an ideal 16:0 SM–16:0 Cer mixture. The *dashed gray line* represents the molecular area for the ideal 16:0 SM (in LC phase)–16:0 Cer mixture. (**c**) Epifluorescence micrographs of pure and mixed 16:0 SM 16:0 SM–16:0 Cer monolayers. The monolayers were doped with 0.5 mol% of the fluorescent probe DiI-C18. All images are 331 × 263 μm in size. Modified from Busto et al. (2009)

A further aspect that deserves some comment is the difference of morphology observed for 16:0 Cer-enriched domains in monolayers. Although small 16:0 Cer concentrations induce segregation in branched domain structures, higher concentrations promote circular and/or peanut-like domain generation. These differences can be understood, according to McConnell's shape transition theory (McConnell 1990), in terms of a competition between two opposing effects, line tension at the domain borders and lateral dipole–dipole repulsion between the coexisting phases. In the presence of 10 mol% 16:0 Cer, domain morphology shows almost circular shapes. By contrast, at 5 mol% 16:0 Cer, round shapes are no longer stable and branched domains of relatively large size are observed (Fig. 2). The latter are likely above the critical area for circular-to-branched shape transition driven by dipolar repulsion within the domain. Morphological changes of Cer-enriched domains where Cer is generated by sphingomyelinase enzymatic activity were described (Fanani et al. 2009). This promotes out-of-equilibrium, high Cer-containing branched domains, whereas subsequent enzyme inactivation induces a change to circular shapes by driving the system toward equilibrium. The stable 16:0 Cer concentration close to 30 mol% within 16:0 Cer-enriched domains appear to reflect near-equilibrium conditions for Cer in mixtures with SM. Small deviations from this concentration cause non-equilibrium conditions and a greater tendency toward branched structures. The observed stable composition ($X_{16:0\ Cer}$ 0.3–0.4) probably reflects the Cer concentration necessary for membrane defects to occur in a specific location, which is, in turn, possibly related to Cer-induced physiological mechanisms [see reviews by Goñi and colleagues; Kolesnick et al. (2000); Cremesti et al. (2002); Goñi and Alonso (2009)].

Mixed films of 2-hydroxy 28:4 Cer with its relative 2-hydroxy 28:4 SM also showed phase separation and formation of Cer-enriched domain (Peñalva et al. 2014). However, the solubility of the VLCPUFA Cer into the SM-enriched phase is larger than that observed for 16:0 Cer/16:0 SM films ($X_{VLCPUFA\ Cer}$ ~0.25 vs. $X_{16:0\ Cer}$ ~0.05). Both the premixed and the enzymatically generated 2-hydroxy 28:4 Cer/28:4 SM films lead to round or worm-like condensed domains. This

effect can be explained as a consequence of a lower difference in the dipole–dipole repulsion between the coexisting phases than that observed in films of 16:0 Cer/16:0 SM. The richer VLCPUFA Cer concentration in the LE phase may have important physiological implications. As commented above, those particular Cers show very large molecular areas in the LE phase, which, combined with a small polar group, result in an inverted cone molecular shape. According to the geometric packing theory (Israelachvili 2011), the enzymatic generation of VLCPUFA Cer promotes the formation of highly curved membranes and vesicle aggregation, an important feature for the acrosomal reaction that takes place in the head of spermatozoa where this kind of lipids abound (Peñalva et al., unpublished).

The phase state of the components appears as a major factor determining miscibility and phase behavior among SMs and Cers even in cases where the lipids have a considerable hydrocarbon chain length mismatch. 16:0 and 24:0 SMs interact favorably in binary mixtures with 10:0, 16:0, 24:0, and 24:1 Cers (Dupuy and Maggio 2014); this is contrary to the binary mixtures of Cers, in which there is a strong dependence of the miscibility on the hydrophobic mismatch between the components (Dupuy and Maggio 2012). The SM/Cer mixtures were characterized by area condensation at low surface pressures and film stiffening at high surface pressures, indicating not only attractive interactions but also complementary accommodation of the molecules at the interface (Dupuy and Maggio 2014). Similar packing interactions were observed in binary mixtures in which one of the components bears a smaller polar head group than the other, such as in the "molecular cavity" effects in mixed films of GM1/Cer (Carrer and Maggio 2001; Maggio 2004) and GM1/dipalmitoyl-PC (Frey et al. 2008).

In mixtures of 16:0 SM with different Cers (10:0, 24:1, and 24:0) at 5 $mN.m^{-1}$, the condensation of the mean molecular area increases linearly with the proportion of Cer, reaching the maximum effect at a proportion of 3:2 (Cer:SM) and remaining essentially invariable thereafter, or even decreasing in the case of the mixture with 10:0 Cer (Fig. 3). This indicates that, at that molar ratio, an optimum packing is reached in which a condensed lattice with enhanced chain interactions occurs. For example, in the case of the mixture 24:1 Cer/16:0 SM in the proportion 3:2 ($X_{Cer} = 0.6$), the mean area condensation at a surface pressure of 3 $mN.m^{-1}$ is 15 $Å^2$, from 58 (ideal value) to 43 $Å^2$ (Fig. 4). Thus, the amount of area condensation of five molecules of SM and Cer in the proportion 3:2 in a mixed film is roughly equivalent to the area occupied by one SM molecule (almost 75 $Å^2$). Lateral condensation in lipid mixtures occurs when a lattice of usually more expanded molecules can accommodate condensed molecules. This is reflected in a negative excess free energy of mixing that usually implies a favorable enthalpic compensation for the entropy loss due to the increased ordering of the molecules

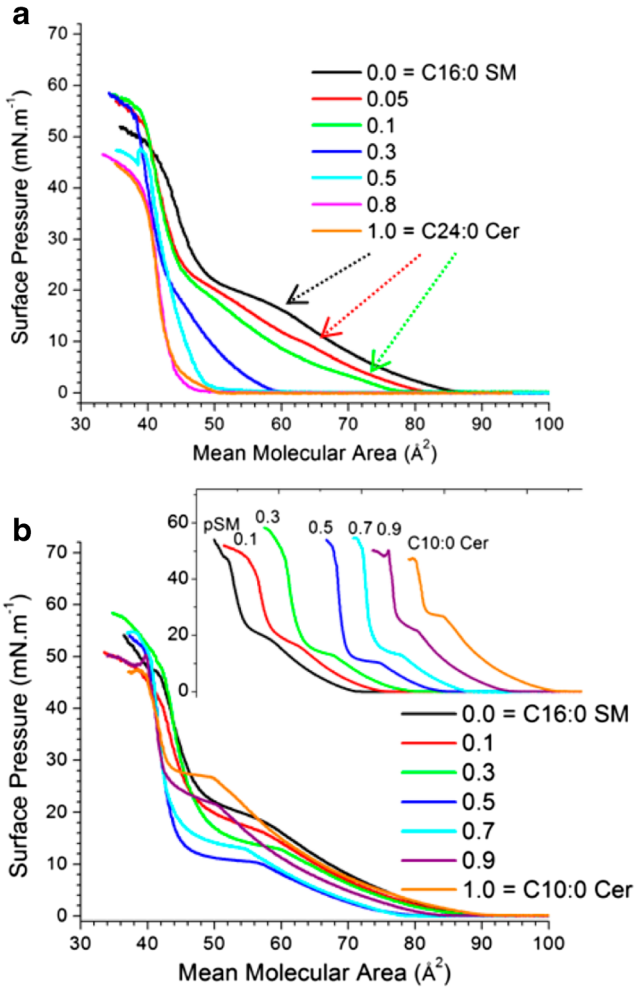

Fig. 3 Compression isotherms of binary mixtures of sphingomyelins and ceramides with a high mismatch in the N-acyl chain length. 12:0 SM/24:0 Cer (**a**) appears rather immiscible, whereas 24:0 SM/10:0 Cer (**b**) formed mixed expanded phases over the whole range of compositions. Reprinted with permission from Dupuy and Maggio (2014). Copyright 2014 American Chemical Society

balancing an unfavorable increased electrostatic repulsion in the crowded array of molecular dipoles.

The mixture formed by 10:0 Cer/16:0 SM provides further insights into the molecular interactions and their effect on the lateral packing in the mixture because, at 5 $mN.m^{-1}$, both the single components and the mixture form expanded phases. The partial mean molecular area contribution of SM in the mixed film was much smaller than its own mean molecular area (80 $Å^2$) at $X_{10:0\ Cer} > 0.4$, reaching a value of 30 $Å^2$ at $X_{10:0\ Cer} = 0.9$ (Fig. 5), which is even less than the value of the cross-sectional area occupied by two closely packed all-trans hydrocarbon chains.

On the other hand, the partial mean molecular area contribution of 10:0 Cer at 5 mN m^{-1} at $X_{10:0\ Cer} = 0.6–0.7$ was also smaller but only by 30% of its own mean molecular area (Fig. 5). The unrealistically smaller partial molecular area contribution of SM to the mean molecular area of the mixture in

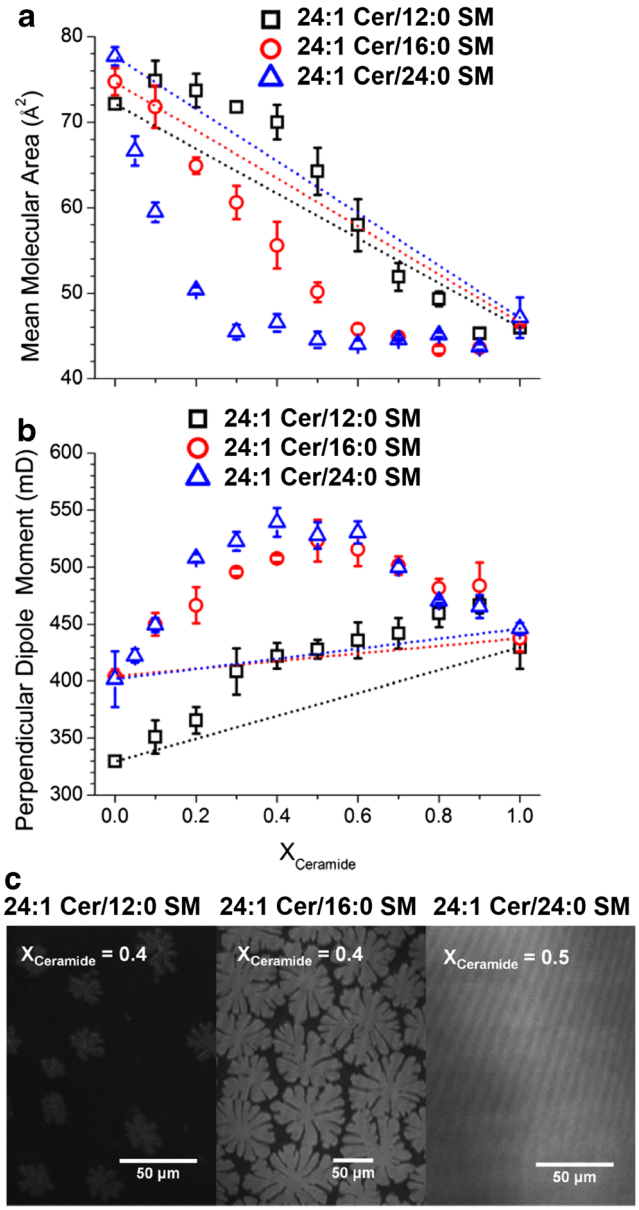

Fig. 4 Variation with the film composition of the mixing parameters: (**a**) mean molecular area, (**b**) perpendicular dipole moment of the binary mixtures of 24:1 Cer with 12:0, 16:0, and 24:0 SM, and (**c**) monolayer imaging by Brewster angle microscopy of the mixtures of 24:1 Cer with 12:0, 16:0, and 24:0 SM at 15 mN m^{-1}. Extracted from Dupuy and Maggio (2014)

Cer-enriched films is due to the strong condensation brought about by the Cer molecules. They can be accommodated in spaces available in the more expanded SM lattice (molecular cavity effect) reflected by the more than 30% area loss of the Cer partial contribution to the mean area of the mixed film. The surface topography of SM/Cer films was affected, not only by an increase of the film optical thickness but also by the consequences of hyperpolarization of the interface (Fig. 4). Condensed domains of large size are formed over the plateau of the compression isotherms of the mixtures that exhibit a transition region (Dupuy and Maggio 2014).

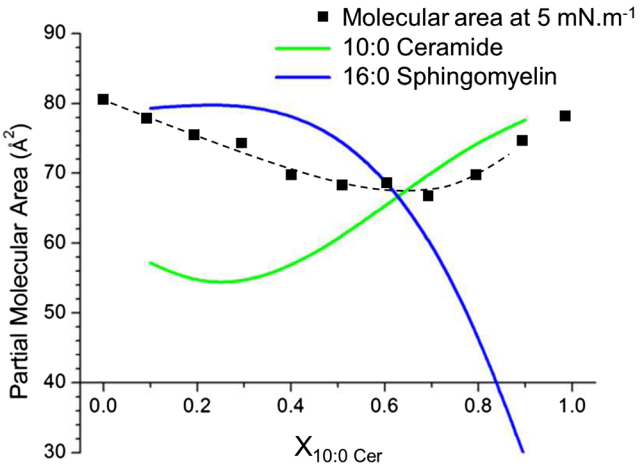

Fig. 5 Partial molecular area contributions of the components of the mixture 10:0 Cer/16:0 SM at 5mN.m^{-1} and at 24 °C. Modified from Dupuy and Maggio (2014)

For example, the mixture 24:1 Cer/16:0 SM shows the largest domains (Fig. 4) when compared to domains formed during the compression of the mixtures of 16:0 SM with either 10:0 or 24:0 Cer (Fig. 6) or with 12:0 SM/24: 1 Cer (Fig. 4). This is in agreement with the degree of hyperpolarization of the perpendicular dipole moment of the different mixtures with respect to the ideal behavior and with the difference between the perpendicular dipole moments of the expanded and

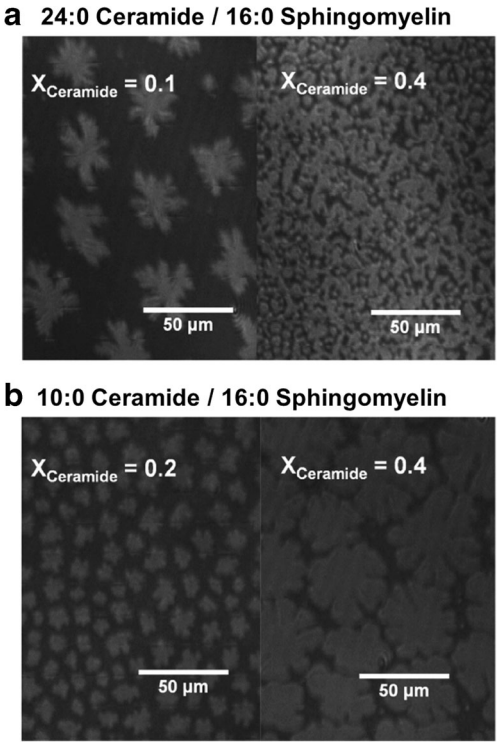

Fig. 6 Monolayer imaging by Brewster angle microscopy of the mixtures at 15 mN.m^{-1} of 16:0 SM with 24:0 Cer (**a**) and 10:0 Cer (**b**). Reprinted with permission from Dupuy and Maggio (2014). Copyright 2014 American Chemical Society

condensed states of each mixture. In fact, the theory for domain shape equilibrium (McConnell 1990; Gutierrez-Campos et al. 2010; Vega Mercado et al. 2012) states that the difference in dipole density between the expanded matrix and the overall dipole of the condensed domains determines that flower-like shapes of increased line tension would form, whereas lower dipole density differences among the segregated condensed and expanded phases should lead to round-shaped domains having a lower line tension.

The mixing behavior of the highly dissimilar lipids 10:0 Cer and 24:0 SM is also in keeping with enhancement of interactions due to complementary packing in an optimal lattice (Dupuy and Maggio 2014). The larger and more hydrated polar head group as well as the asymmetry of the acyl chains both impair a tight packing of SM molecules, yielding an expanded matrix in which Cer with a smaller polar group can be accommodated. On the other hand, the asymmetric 10:0 Cer, due to the shorter N-acyl chain, can also form films in the expanded state, depending on the surface pressure. A difference of eight carbons in the N-acyl chain length between the sphingoid and N-acyl chains in the molecules leads to complete immiscibility, whereas mixed films of condensed Cers with a mismatch of just four carbons forms mixed expanded phases (for example, 14:0/10:0 Cers or 16:0/12:0 Cers) (Dupuy and Maggio 2012). This is in agreement with the overall results because, in the case of mixing lipids of the same kind, the phase state of a lipid correlates with the length of the N-acyl chains, and the dependence of the mixing behavior with the hydrophobic mismatch between components is directly related to differences of their phase state.

Even though the hydrophobic mismatch between the components of the mixtures 24:0 Cer/12:0 SM and 10:0 Cer/24:0 SM differ by only two methylene groups, the difference in the phase state between a long chain Cer (very condensed) and a short chain SM (expanded) is much larger than in the case of a short chain Cer (less condensed) and a long chain SM (less expanded). This can explain why a highly condensed lattice formed by the long chain Cer prevents miscibility with the short chain expanded SM, whereas the more expanded short chain Cer allows mixing with a more condensed long chain SM over the whole range of composition.

Ceramide–glycosphingolipid interactions

On biochemical terms, biosynthetic pathways of GSLs include increased glycosylation of Cer by selective enzymes that establish biosynthetic diversion points for sequences of substrate–product relationships of GSLs with different oligosaccharide chain complexity [for further references, see Maccioni et al. (2002); Yu et al. (2004)]. At the membrane level, such a rather complex biocatalytic pattern further introduces an important physico-chemical problem related to the favorable or unfavorable thermodynamic tendency for mixing among precursor–product GSLs having marked differences in their molecular packing, surface electrostatic, and phase state. Rather thorough reviews on the biophysical behavior of a considerable number of GSLs of different complexity are available in the literature (Maggio 1994; Maggio et al. 2004, 2006, 2008).

The presence of a lactose moiety in the polar head group works against homo-association and actually weakens intermolecular interactions by reducing packing efficiency (Regen 2002). This questions the common misunderstanding that hydrogen bonding among glycolipids could be an initial driving force for their self-segregation. On the contrary, further glycosylation in the polar head group of the more complex GSLs further decreases intermolecular cohesion, a consequence of more favorable hydrogen bonding to water in the oligosaccharide hydration shell (Bianco et al. 1988). Moreover, the complete phase diagrams of more than 11 binary mixtures with DPPC showed that segregation of domains enriched in GSLs is due to the *phospholipid* tendency to exclude the latter and not to the self-segregation of the former (Maggio et al. 1985).

Mixed films of Cer and neutral GSLs with short oligosaccharide chains show non-ideal mixing behavior and expansion of the mean molecular area at all surface pressures. This is accompanied by positive deviations from ideality of the average surface potential per unit of molecular surface density (commonly denominated surfaced potential/molecule), indicating molecular dipole hyperpolarization and intermolecular repulsion in the mixed films (Fig. 7a). In spite of the area expansion, the in-plane (Gibbs) elasticity of the film is rather high (relatively large values of the compressibility modulus K over the whole range of mean molecular areas) compared to that of ideal mixtures; this indicates that molecular hyperpolarization imposes interfacial rigidity which reduces the liquid-expanded character, together with an increase of intermolecular separation due to dipolar repulsion (Maggio 2004). A conspicuous change of behavior occurs in mixtures of Cer with GSLs having more than three carbohydrate units. Compared to ideal monolayers, the mixed films are slightly expanded at low surface pressures but condensation of the mean molecular area can be observed at high lateral pressures (Fig. 7b). In spite of intermolecular condensation, the interface remains slightly hyperpolarized, with the in-plane elasticity above (larger K values) that of the ideal mixture (Maggio 2004).

Mixed films of Cer with ganglioside GM3 [the simplest ganglioside, and a key point for diversion of enzymatic routes for ganglioside biosynthesis (Maccioni et al. 2002; Yu et al. 2004)] show molecular area condensation (Fig. 7c) with ideal behavior of the surface potential/molecule. This suggests a "molecular cavity" effect (Maggio et al. 1997; Carrer and Maggio 2001; Diociaiuti et al. 2004), consistent with reduction of the mean molecular area with essentially unchanged dipolar properties of the lipids and of the film elasticity

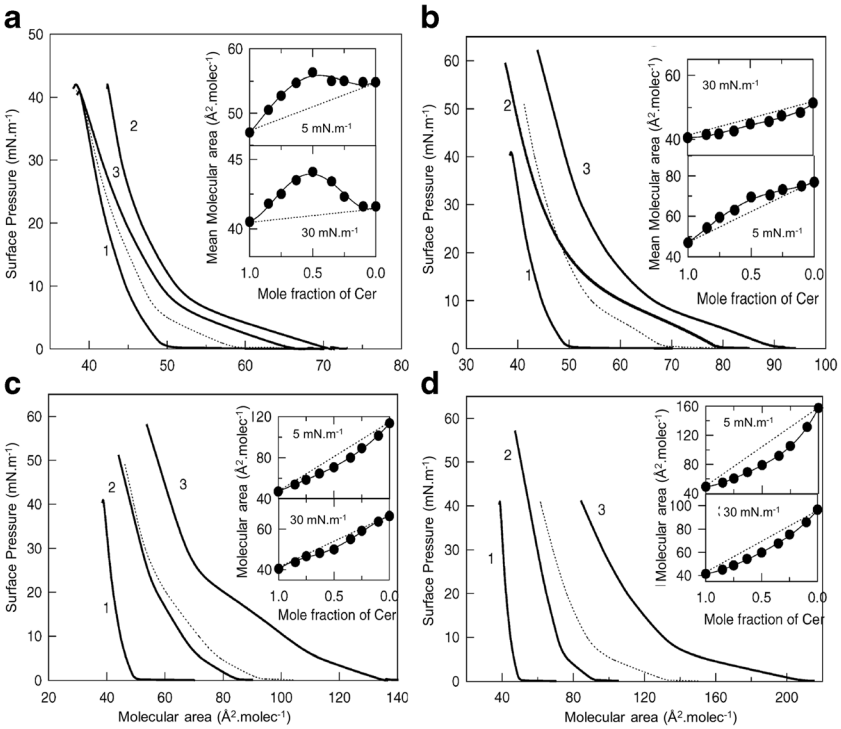

Fig. 7 The surface pressure–molecular area isotherms of mixed monolayers of ceramide and glycosphingolipids or gangliosides: (**a**) mixed films of ceramide and GlcCer; (**b**) ceramide and Gg4cCer; (**c**) ceramide and GM3; and (**d**) ceramide and GD1a. The insets show the deviation from the ideal behavior (*dashed straight line*) of the mean molecular area at the surface pressure indicated for the mixed films in the proportions shown in the abscissa. Extracted from Maggio (2004)

compared to an ideally mixed film. The interactions of Cer with ganglioside GD3, located at a further diversion point in the biosynthetic pathway of complex gangliosides (Maccioni et al. 2002; Yu et al. 2004), are similar to those of mixtures with GM3 (Fig. 7c). With more complex gangliosides, the mixed films with Cer exhibit condensation of the mean molecular area and interfacial depolarization (Fig. 7d). The increase in polar head group complexity of the ganglioside (in the series GM2, GM1, GD1a, and GT1b) brings about an increase of the magnitude of molecular condensation, depolarization, and an increasingly reduced in-plane elasticity compared to the ideally mixed films (Maggio 2004).

The variation of mean molecular area and average surface potential/molecule, with respect to the ideal behavior, in a binary monolayer can be due to changes of the molecular parameters of one, the other, or both lipid components (Maggio et al. 1997; Carrer and Maggio 2001). At constant (low or high) surface pressure, the contribution of Cer to the cross-sectional molecular area and surface potential/molecule in mixed monolayer with GlcCer at high proportions of Cer do not show large changes compared to the area contribution in pure Cer films (Fig. 8a). On the other hand, significant increases of those parameters occur at high proportions of GlcCer. Similarly, the area and surface potential/molecule contributions of GlcCer are increased at high proportions of Cer compared to pure films of GlcCer (Fig. 8d). This behavior is essentially similar in mixed films of Cer with LacCer.

In mixtures of Cer with Gg4Cer, having a longer neutral oligosaccharide chain, a different behavior is observed at low compared to high surface pressures (Fig. 8b). At low surface pressures, the contributions to the mean molecular area and average surface potential/molecule in the mixed films are similar to those described above for films of Cer and GlcCer. However, at high surface pressures, the molecular area contribution to that of the mixture is decreased for either Cer or Gg4Cer in films enriched, respectively, with the other component. The variation with the film composition of the contribution of the partial surface potential/molecule of each lipid at high surface pressure follows the same trend as at low pressures when the proportion of the other lipid in the mixture is high.

Mixed films of Cer and GD1a exemplify the behavior found in mixtures with the more complex gangliosides (Fig. 8c). The molecular area contribution of Cer in mixed films with a high proportion of GD1a is not changed, either at low or high surface pressures, and is similar to that in films of pure Cer. On the other hand, in films with increasing proportions of ganglioside, the Cer contribution to the mean molecular area of the mixture is, at first, greatly reduced and then it no longer contributes to the film area and its partial molecular area can even acquire negative values (Maggio 2004). This indicates that Cer becomes "sequestered" in surface defects due to irregular lateral packing in the two-dimensional ganglioside-enriched lattice (Carrer and Maggio 2001; Rosetti et al. 2003; Maggio 2004). The films are non-ideal, exhibiting strong condensation and depolarization that reveals molecular interactions and "miscibility" on the nm scale range according to the additivity rule. However, on the μm scale range, these

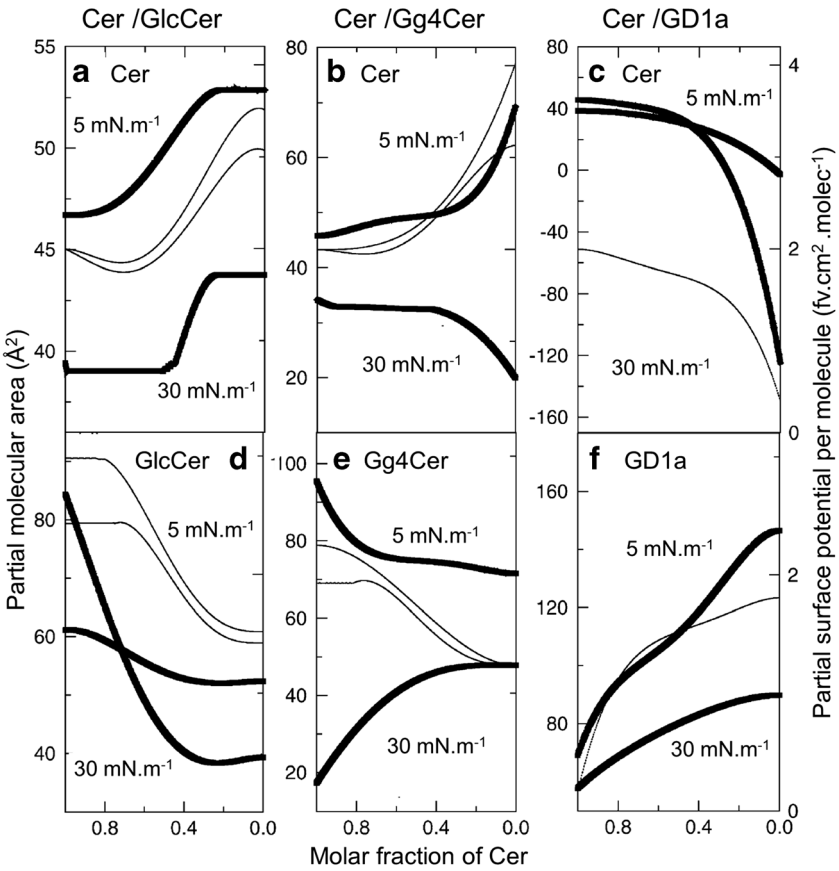

Fig. 8 Variation of partial mean molecular area and average surface potential/molecule with the films composition in mixed monolayers of ceramide with GSLs. The variation of the partial mean molecular area (*thick lines*) or the partial average surface potential/molecule (*thin lines*) of ceramide (**a**–**c**) in the presence of GlcCer (**d**), Gg4Cer (**e**), or ganglioside GD1a (**f**) is shown for mixed films with the proportions of ceramide indicated in the abscissa. As indicated in each panel, the surface pressures points at which the values were derived for both parameters correspond to 5 $mN.m^{-1}$ (*upper curves*) and 30 $mN.m^{-1}$ (*lower curves*); in **c** and **f**, the curves for the surface potential/molecule (*thin lines*) at 5 and 30 $mN.m^{-1}$ are essentially superimposed. Reprinted from Maggio (2004), copyright 2004, with permission from Elsevier

films show coexistence of condensed Cer-enriched and liquid-expanded GM1-enriched domains in a microheterogeneous topography that can be visually observed along the lateral plane (Rosetti et al. 2003). This is, again, another example where a large amount of lateral interface establishes domain line tensions and super-lattice structuring that blur away intermolecular cooperativity on the short range, thus resulting in smooth compression isotherms. In addition, the average optical thickness of these interfaces, at least at surface pressures above 20 $mN.m^{-1}$, is increased compared to that found in pure Cer films, which can be mostly accounted for by the protrusion of the ganglioside oligosaccharide chain perpendicularly into the aqueous subphase (Rosetti et al. 2003).

In bulk dispersions, the Cer–ganglioside interactions in the two-dimensional plane can be further transduced to thermodynamic–geometric compensation escaping into the third dimension, which affects the phase state and topology of the self-assembled structure (Carrer and Maggio 2001). In the mixed films, the contribution of Cer to the surface potential/molecule progressively diminishes as the content of ganglioside is increased: it abruptly decreases to very low values at high ganglioside proportions, indicating strong lipid depolarization in these conditions. In turn, the molecular area contribution of the ganglioside in the mixed film is gradually decreased as the proportion of Cer increases, while the surface potential/molecule contribution results in the film being gradually depolarized [Fig. 8 and Maggio (2004)]. The molecular area contributions to that of the mixed monolayer of GD1a or GT1b with Cer are greatly reduced. However, the cross-sectional area contribution of these gangliosides does not reach values as small as those observed for the molecular area contribution of GM1, namely about 35 $Å^2$ (Carrer and Maggio 2001), which is about the minimum possible for two closely packed hydrocarbon chains perpendicular to the interface. This is consistent with previous reports indicating that the extended oligosaccharide chain of gangliosides and other GSLs, oriented perpendicularly to the interface (Maggio et al. 1978b, 1981; Li et al. 2002; Diociaiuti et al. 2004), can largely "fit" under the area of two closely packed hydrocarbon chains. For the more complex oligosaccharide polar head groups, slightly more spacing is required, especially at low surface pressures (Maggio et al. 1981; Carrer and Maggio 2001).

The compression free energy (the two-dimensional work required to bring together the GSL molecules from the liquid-expanded state to a closely packed state) increases in an approximately linear fashion. This indicates that it is increasingly more difficult to closely pack these lipids as they contain more complex polar head groups (Fig. 9a) due to steric, dipole moment and electrostatic charge repulsion, and hydration–

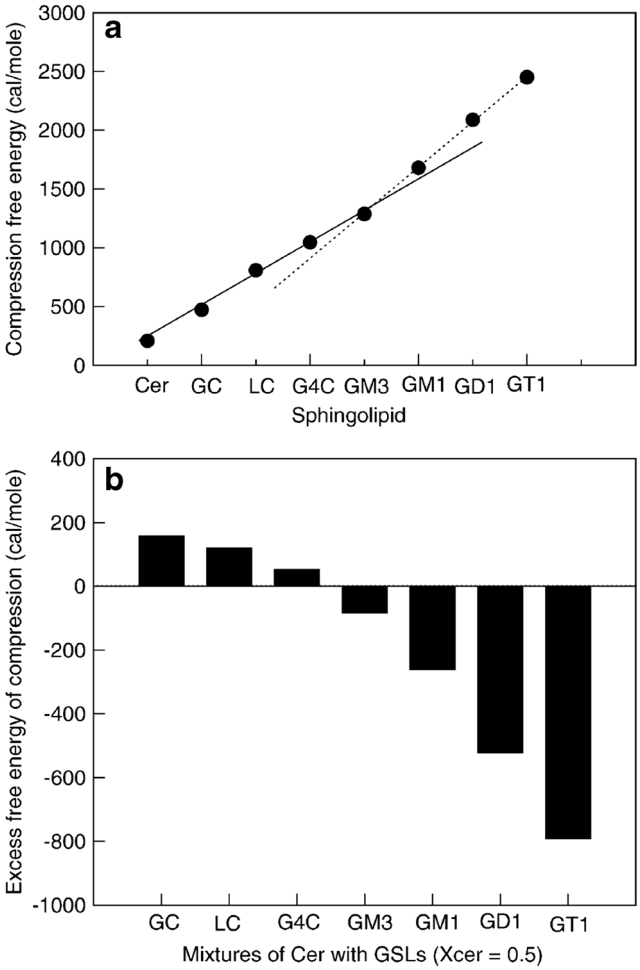

Fig. 9 Variation of compression free energy in monolayers of GSLs and excess free energy of compression in mixed films with ceramide. The free energy of compression between 2 and 35 $mN.m^{-1}$ of the sphingolipid indicated in the abscissa is shown in (**a**). The variation with the type of oligosaccharide chain in the GSLs can be described by two regression lines with different slopes for the series of neutral GSLs (267 cal/mol/carbohydrate residue, $r^2 = 0.995$) and gangliosides (390 cal/mol/carbohydrate residue, $r^2 = 0.999$).The excess free energy of compression for films of the GSLs indicated in the abscissa with ceramide in equimolar proportions is shown in (**b**). Reprinted from Maggio (2004), copyright 2004, with permission from Elsevier

dehydration effects mediated by the complexity of the polar head group and the coalescence of the oligosaccharide hydration shell. This occurs with the release of interfacial water, balanced by cohesive interactions among the hydrocarbon chains beyond a certain proximity (Maggio et al. 1981; Bianco et al. 1988). The sign and magnitude of the excess free energy of compression (the difference between the compression free energy of the mixed film and that of the corresponding ideal mixture in which mixing results solely from entropic effects) reflects how favorable are the lipid–lipid interactions. As an example, the excess free energy of compression of films containing Cer becomes progressively more favorable as the oligosaccharide chain of the GSLs in the binary mixture is more complex (Fig. 9b).

General summary

The capability of even a single type of Cer or SM to induce formation of solid-like segregated domains, with effects on the more liquid-like regions of membranes, should not be considered lightly, but only after strictly defining the type of N-linked acyl chain composition involved and how the components mix among themselves. The most common Cers in biological systems, 16:0 Cer, is not completely solid, different to what is usually conceived, but it displays a rich phase coexistence even over the physiological temperature range (see also Part I of this Special Issue). At low temperature, middle long Cer monolayers behave as very rigid solid films, displaying viscoelastic features (López-Montero et al. 2013). However, this condition changes upon heating of a few degrees. Above the physiological temperature, a softened solid or LC phase is observed (Fanani and Maggio 2010; Catapano et al. 2015), and a further increase in temperature shows the presence of LE monolayers. On the other hand, Cers with shorter chains can also form expanded mixed phases, depending on the surface pressure. It is worth recalling that the average lateral surface pressure in biomembranes largely fluctuates (even by more than ± 15 $mN.m^{-1}$), depending on the thermal energy and film elasticity, especially when phase coexistence occurs (Phillips et al. 1975). Thus, transient mixing–demixing processes among different Cer species continuously occur in biomembranes, both inside Cer-enriched rigid domains or platforms as well as in the expanded phase, which may regulate lateral partitioning of lipids and proteins. The results described highlight the rich complexity of mixing–demixing phenomena involving Cers which is usually neglected but should be taken into account when considering structure-mediated signaling in biomembranes (van Blitterswijk et al. 2003).

The phase state of the components appears as a major factor determining miscibility and phase behavior among SMs and Cers, even in cases where the lipids have a considerable hydrocarbon chain length mismatch. The two-dimensional mixing of the simpler sphingolipids bearing different hydrocarbon moieties is quite complex, similar to the polar headgroup-driven miscibility among the more complex glycosphingolipids bearing different oligosaccharide chains (Maggio 2004). Molecular cavity effects and critical lattice distortion not only cause lateral reorganization in terms of the segregation of condensed domains but also have far-reaching consequences for the molecular packing, surface hyperpolarization, and elasticity of the interface. These features can also modulate protein insertion and enzyme activities (Maggio et al. 2008), such as dipole potential- and packing-sensitive lipases PLA2 (Perillo et al. 1994; Maggio 1999).

The mixing behavior of different species of Cers and SMs in terms of their N-acyl chain shows that "Cer-enriched domains" present in an expanded membrane should still behave

as solid platforms with important biological implications. However, it cannot be simply conceived as highly condensed and phase-segregated only on the basis of the properties of the more commonly studied Cer analogs and then extrapolated to all types of Cer mixtures, let alone natural membranes. SMs show a more expanded behavior than Cers N-acylated with the same fatty acyl chains, and both types of lipids interacted favorably in monolayers at the air−water interface, even in the presence of considerable hydrocarbon chain length mismatch. The complementary packing between these sphingolipids leads to mean area condensation and film stiffening accompanied by hyperpolarization and optical thickening of the interface in most of the mixtures. The optimal packing of the components in the mixtures enhanced molecular interactions necessary to counterbalance increased dipolar repulsions, indicating that the ordering in the hydrocarbon region is a major factor influencing the mixing behavior of different species of SM and Cer.

Surface miscibility depends more on the phase state of the major component than on the hydrophobic mismatch in the acyl chain lengths. Total immiscibility could be observed only in the case of the mixture between a short chain SM (12:0 SM, fully expanded monolayer) and a long chain Cer (24:0 Cer, fully condensed monolayer). The fact that long chain Cers such as 24:0 and 24:1, but not 16:0 Cer, can form mixed expanded phases with different SMs as a consequence of the acyl chain disorder introduced by the relative asymmetry of the length of the hydrocarbon chains and the resulting overall phase state is a novel finding in the field of membrane biophysics of sphingolipids that challenges the common idea of Cers as only being a solid domain-forming lipid.

The partial molecular properties in the binary mixtures of Cer and GSLs exhibit, in general, the following trend. In mixed monolayers exhibiting mean molecular area expansion, the area contribution of each component is individually increased in films containing a high proportion of the other; at the same time, the surface potential/molecule contribution of each lipid indicates hyperpolarization. In films exhibiting condensation of the mean molecular area, the contribution of the more expanded lipid (usually the one with the more complex oligosaccharide chain) undergoes progressive reduction as the proportion of the more condensed GSLs increases in the mixed film. On the other hand, the partial molecular area and partial surface potential/molecule contributions to the mixture of the more condensed GSLs remain relatively unchanged until high proportions of the more expanded component are reached. After this, its contribution to the properties of the mixed film becomes markedly reduced and, in mixtures of the simplest GSLs with those having complex polar head groups, can even acquire negative values due to its sequestration in a lattice exhibiting molecular cavity effects. The likelihood for lateral packing defects in the two-dimensional lattice increases with the polar head group complexity and, when the oligosaccharide chain of two GSLs in the mixture is either relatively large or small compared to the other "molecular cavity", effects occur. It is increasingly more difficult to closely pack GSLs as they contain more complex polar head groups due to steric, dipole moment and electrostatic charge repulsion, and hydration–dehydration effects.

As a concluding remark, it is worth pointing out that the miscibility capacity of the sphingolipids discussed in this revision work influence the overall lateral structure and membrane texture at the mesoscale level, as well as the topological structure of the three-dimensional organization of the membrane. Thus, changes in composition due to enzymatic activity, fluctuations of surface pressure, and/or electrostatic effects have the potential of changing the miscibility properties and, by extension, the overall membrane structure.

Acknowledgements This work was supported by the Consejo Nacional de Investigaciones Científicas y Técnicas (CONICET), Agencia Nacional de Promoción Científica y Tecnológica (ANPCyT, FONCyT PICT 2014-1627), and the Secretary of Science and Technology of Universidad Nacional de Córdoba (SECyT-UNC), Argentina.

Compliance with ethical standards

Conflict of interest María Laura Fanani declares that she has no conflicts of interest. Bruno Maggio declares that he has no conflicts of interest.

Ethical approval This article does not contain any studies with human participants or animals performed by any of the authors.

References

Ale EC, Maggio B, Fanani ML (2012) Ordered-disordered domain coexistence in ternary lipid monolayers activates sphingomyelinase by clearing ceramide from the active phase. Biochim Biophys Acta Biomembr 1818:2767–2776

Arriaga LR, López-Montero I, Ignés-Mullol J, Monroy F (2010) Domain-growth kinetic origin of nonhorizontal phase coexistence plateaux in langmuir monolayers: compression rigidity of a raft-like lipid distribution. J Phys Chem B 114:4509–4520. doi:10.1021/jp9118953

Bianco ID, Fidelio GD, Maggio B (1988) Effect of glycerol on the molecular properties of cerebrosides, sulphatides and gangliosides in monolayers. Biochem J 251:613–616

Brockman H (1994) Dipole potential of lipid membranes. Chem Phys Lipids 73:57–79. doi:10.1016/0009-3084(94)90174-0

Busto JV, Fanani ML, De Tullio L et al (2009) Coexistence of immiscible mixtures of palmitoylsphingomyelin and palmitoylceramide in monolayers and bilayers. Biophys J 97:2717–2726. doi:10.1016/j.bpj.2009.08.040

Busto JV, Sot J, Requejo-Isidro J, Goñi FM, Alonso A (2010) Cholesterol displaces palmitoylceramide from its tight packing with palmitoylsphingomyelin in the absence of a liquid-disordered phase. Biophys J 99:1119–1128. doi:10.1016/j.bpj.2010.05.032

Carrer DC, Maggio B (1999) Phase behavior and molecular interactions in mixtures of ceramide with dipalmitoylphosphatidylcholine. J Lipid Res 40:1978–1989

Carrer DC, Maggio B (2001) Transduction to self-assembly of molecular geometry and local interactions in mixtures of ceramides and ganglioside GM1. Biochim Biophys Acta Biomembr 1514:87–99. doi:10.1016/S0005-2736(01)00366-2

Carrer DC, Schreier S, Patrito M, Maggio B (2006) Effects of a short-chain ceramide on bilayer domain formation, thickness, and chain mobililty: DMPC and asymmetric ceramide mixtures. Biophys J 90:2394–2403. doi:10.1529/biophysj.105.074252

Castro BM, de Almeida RFM, Silva LC, Fedorov A, Prieto M (2007) Formation of ceramide/sphingomyelin gel domains in the presence of an unsaturated phospholipid: a quantitative multiprobe approach. Biophys J 93:1639–1650. doi:10.1529/biophysj.107.107714

Catapano ER, Arriaga LR, Espinosa G, Monroy F, Langevin D, López-Montero I (2011) Solid character of membrane ceramides: a surface rheology study of their mixtures with sphingomyelin. Biophys J 101:2721–2730. doi:10.1016/j.bpj.2011.10.049

Catapano ER, Lillo MP, García Rodríguez C et al (2015) Thermomechanical transitions of egg-ceramide monolayers. Langmuir 31:3912–3918. doi:10.1021/acs.langmuir.5b00229

Chiantia S, Ries J, Chwastek G et al (2008) Role of ceramide in membrane protein organization investigated by combined AFM and FCS. Biochim Biophys Acta Biomembr 1778:1356–1364. doi:10.1016/j.bbamem.2008.02.008

Contreras FX, Villar AV, Alonso A, Kolesnick RN, Goñi FM (2003) Sphingomyelinase activity causes transbilayer lipid translocation in model and cell membranes. J Biol Chem 278:37169–37174. doi:10.1074/jbc.M303206200

Cremesti AE, Goni FM, Kolesnick R (2002) Role of sphingomyelinase and ceramide in modulating rafts: do biophysical properties determine biologic outcome? FEBS Lett 531:47–53. doi:10.1016/S0014-5793(02)03489-0

de Almeida RFM, Loura LMS, Fedorov A, Prieto M (2005) Lipid rafts have different sizes depending on membrane composition: a time-resolved fluorescence resonance energy transfer study. J Mol Biol 346:1109–1120. doi:10.1016/j.jmb.2004.12.026

De Tullio L, Maggio B, Fanani ML (2008) Sphingomyelinase acts by an area-activated mechanism on the liquid-expanded phase of sphingomyelin monolayers. J Lipid Res 49:2347–2355. doi:10.1194/jlr.M800127-JLR200

Diociaiuti M, Ruspantini I, Giordani C, Bordi F, Chistolini P (2004) Distribution of GD3 in DPPC monolayers: a thermodynamic and atomic force microscopy combined study. Biophys J 86:321–328. doi:10.1016/S0006-3495(04)74107-7

Dupuy F, Fanani ML, Maggio B (2011) Ceramide N-acyl chain length: a determinant of bidimensional transitions, condensed domain morphology, and interfacial thickness. Langmuir 27:3783–3791

Dupuy F, Maggio B (2012) The hydrophobic mismatch determines the miscibility of ceramides in lipid monolayers. Chem Phys Lipids 165:615–629. doi:10.1016/j.chemphyslip.2012.06.008

Dupuy FG, Maggio B (2014) N-acyl chain in ceramide and sphingomyelin determines their mixing behavior, phase state, and surface topography in Langmuir films. J Phys Chem B 118:7475–7487. doi:10.1021/jp501686q

Fanani ML, De Tullio L, Hartel S, Jara J, Maggio B (2009) Sphingomyelinase-induced domain shape relaxation driven by out-of-equilibrium changes of composition. Biophys J 96:67–76. doi:10.1529/biophysj.108.141499

Fanani ML, Härtel S, Oliveira RG, Maggio B (2002) Bidirectional control of sphingomyelinase activity and surface topography in lipid monolayers. Biophys J 83:3416–3424

Fanani ML, Maggio B (2010) Phase state and surface topography of palmitoyl-ceramide monolayers. Chem Phys Lipids 163:594–600

Frey SL, Chi EY, Arratia C, Majewski J, Kjaer K, Lee KY (2008) Condensing and fluidizing effects of ganglioside GM1 on phospholipid films. Biophys J 94:3047–3064. doi:10.1529/biophysj.107.119990

Goñi FM, Alonso A (2006) Biophysics of sphingolipids I. Membrane properties of sphingosine, ceramides and other simple sphingolipids. Biochim Biophys Acta Biomembr 1758:1902–1921. doi:10.1016/j.bbamem.2006.09.011

Goñi FM, Alonso A (2009) Effects of ceramide and other simple sphingolipids on membrane lateral structure. Biochim Biophys Acta Biomembr 1788:169–177. doi:10.1016/j.bbamem.2008.09.002

Gutierrez-Campos A, Diaz-Leines G, Castillo R (2010) Domain growth, pattern formation, and morphology transitions in Langmuir monolayers. A new growth instability. J Phys Chem B 114:5034–5046. doi:10.1021/jp910344h

Härtel S, Fanani ML, Maggio B (2005) Shape transitions and lattice structuring of ceramide-enriched domains generated by sphingomyelinase in lipid monolayers. Biophys J 88:287–304. doi:10.1529/biophysj.104.048959

Heerklotz H (2008) Interactions of surfactants with lipid membranes. Q Rev Biophys 41:205–264. doi:10.1017/S0033583508004721

Hertz R, Barenholz Y (1975) Permeability and integrity properties of lecithin-sphingomyelin liposomes. Chem Phys Lipids 15:138–156. doi:10.1016/0009-3084(75)90037-7

Holopainen JM, Brockman HL, Brown RE, Kinnunen PK (2001) Interfacial interactions of ceramide with dimyristoylphosphatidylcholine: impact of the N-acyl chain. Biophys J 80:765–775. doi:10.1016/S0006-3495(01)76056-0

Hsueh Y-W, Giles R, Kitson N, Thewalt J (2002) The effect of ceramide on phosphatidylcholine membranes: a deuterium NMR study. Biophys J 82:3089–3095. doi:10.1016/S0006-3495(02)75650-6

Huang HW, Goldberg EM, Zidovetzki R (1996) Ceramide induces structural defects into phosphatidylcholine bilayers and activates phospholipase A2. Biochem Biophys Res Commun 220:834–838. doi:10.1006/bbrc.1996.0490

Israelachvili JN (2011) Soft and biological structures. In: Israelachvili JN (ed) Intermolecular and surface forces, 3rd edn. Academic Press, San Diego, CA, pp 535–576

Karttunen M, Haataja MP, Säily M, Vattulainen I, Holopainen JM (2009) Lipid domain morphologies in phosphatidylcholine—ceramide monolayers. Langmuir 25:4595–4600. doi:10.1021/la803377s

Kolesnick RN, Goñi FM, Alonso A (2000) Compartmentalization of ceramide signaling: physical foundations and biological effects. J Cell Physiol 184:285–300

Leung SSW, Busto JV, Keyvanloo A, Goñi FM, Thewalt J (2012) Insights into sphingolipid miscibility: separate observation of sphingomyelin and ceramide N-acyl chain melting. Biophys J 103:2465–2474. doi:10.1016/j.bpj.2012.10.041

Li X-M, Momsen MM, Brockman HL, Brown RE (2002) Lactosylceramide: effect of acyl chain structure on phase behavior and molecular packing. Biophys J 83:1535–1546. doi:10.1016/S0006-3495(02)73923-4

López-Montero I, Catapano ER, Espinosa G, Arriaga LR, Langevin D, Monroy F (2013) Shear and compression rheology of Langmuir monolayers of natural ceramides: solid character and plasticity. Langmuir 29:6634–6644. doi:10.1021/la400448x

López-Montero I, Monroy F, Vélez M, Devaux PF (2010) Ceramide: from lateral segregation to mechanical stress. Biochim Biophys Acta Biomembr 1798:1348–1356. doi:10.1016/j.bbamem.2009.12.007

Mabrey S, Sturtevant JM (1976) Investigation of phase transitions of lipids and lipid mixtures by sensitivity differential scanning calorimetry. Proc Natl Acad Sci U S A 73:3862–3866

Maccioni HJF, Giraudo CG, Daniotti JL (2002) Understanding the stepwise synthesis of glycolipids. Neurochem Res 27:629–636. doi:10.1023/A:1020271932760

Maggio B (1999) Modulation of phospholipase A2 by electrostatic fields and dipole potential of glycosphingolipids in monolayers. J Lipid Res 40:930–939

Maggio B (2004) Favorable and unfavorable lateral interactions of ceramide, neutral glycosphingolipids and gangliosides in mixed monolayers. Chem Phys Lipids 132:209–224. doi:10.1016/j.chemphyslip.2004.07.002

Maggio B (1994) The surface behavior of glycosphingolipids in biomembranes: a new frontier of molecular ecology. Prog Biophys Mol Biol 62:55–117. doi:10.1016/0079-6107(94)90006-X

Maggio B, Ariga T, Calderón RO, Yu RK (1997) Ganglioside GD3 and GD3-lactone mediated regulation of the intermolecular organization in mixed monolayers with dipalmitoylphosphatidylcholine. Chem Phys Lipids 90:1–10. doi:10.1016/S0009-3084(97)00090-X

Maggio B, Ariga T, Sturtevant JM, Yu RK (1985) Thermotropic behavior of glycosphingolipids in aqueous dispersions. Biochemistry 24:1084–1092

Maggio B, Borioli GA, Del Boca M et al (2008) Composition-driven surface domain structuring mediated by sphingolipids and membrane-active proteins: above the nano- but under the microscale: Mesoscopic biochemical/structural cross-talk in biomembranes. Cell Biochem Biophys 50:79–109. doi:10.1007/s12013-007-9004-1

Maggio B, Carrer DC, Fanani ML, Oliveira RG, Rosetti CM (2004) Interfacial behavior of glycosphingolipids and chemically related sphingolipids. Curr Opin Colloid Interface Sci 8:448–458

Maggio B, Cumar FA, Caputto R (1978a) Interactions of gangliosides with phospholipids and glycosphingolipids in mixed monolayers. Biochem J 175:1113–1118

Maggio B, Cumar FA, Caputto R (1978b) Surface behaviour of Gangliosides and related glycosphingolipids. Biochem J 171:559–565

Maggio B, Cumar FA, Caputto R (1981) Molecular behaviour of glycosphingolipids in interfaces. Possible participation in some properties of nerve membranes. Biochim Biophys Acta 650:69–87

Maggio B, Fanani ML, Rosetti CM, Wilke N (2006) Biophysics of sphingolipids II. Glycosphingolipids: an assortment of multiple structural information transducers at the membrane surface. Biochim Biophys Acta Biomembr 1758:1922–1944

McConnell HM (1990) Harmonic shape transitions in lipid monolayer domains. J Phys Chem 94:4728–4731

Möhwald H (1995) Phospholipid monolayers. In: Lipowsky R, Sackmann E (eds) Structure and dynamics of membranes A. Elsevier Science B.V., Amsterdam, pp 161–211

Oliveira RG, Maggio B (2000) Epifluorescence microscopy of surface domain microheterogeneity in myelin monolayers at the air–water interface. Neurochem Res 25:77–86. doi:10.1023/A:1007591516539

Oliveira RG, Maggio B (2002) Compositional domain immiscibility in whole myelin monolayers at the air–water interface and Langmuir–Blodgett films. Biochim Biophys Acta Biomembr 1561:238–250. doi:10.1016/S0005-2736(02)00350-4

Patra SK, Alonso A, Arrondo JLR, Goñi FM (1999) Liposomes containing sphingomyelin and cholesterol: detergent solubilisation and infrared spectroscopic studies. J Liposome Res 9:247–260. doi:10.3109/08982109909024788

Patra SK, Alonso A, Goñi FM (1998) Detergent solubilisation of phospholipid bilayers in the gel state: the role of polar and hydrophobic forces. Biochim Biophys Acta Biomembr 1373:112–118. doi:10.1016/S0005-2736(98)00095-9

Peñalva DA, Wilke N, Maggio B, Aveldaño MI, Fanani ML (2014) Surface behavior of sphingomyelins with very long chain polyunsaturated fatty acids and effects of their conversion to ceramides. Langmuir 30:4385–4395. doi:10.1021/la500485x

Perillo MA, Guidotti A, Costa E, Yu RK, Maggio B (1994) Modulation of phospholipases A2 and C activities against dilauroylphosphorylcholine in mixed monolayers with semisynthetic derivatives of ganglioside and sphingosine. Mol Membr Biol 11:119–126. doi:10.3109/09687689409162229

Phillips MC (1972) The physical state of phospholipids and cholesterol in monolayers, bilayers, and membranes. In: Danielli JF, Rosenberg MD, Cadenhead DA (eds) Progress in surface and membrane science. Academic Press, New York, pp 139–221

Phillips MC, Graham DE, Hauser H (1975) Lateral compressibility and penetration into phospholipid monolayers and bilayer membranes. Science 254:154–156

Pilar Veiga M, Arrondo JLR, Goñi FM, Alonso A, Marsh D (2001) Interaction of cholesterol with sphingomyelin in mixed membranes containing phosphatidylcholine, studied by spin-label ESR and IR spectroscopies. A possible stabilization of gel-phase sphingolipid domains by cholesterol. Biochemistry 40:2614–2622. doi:10.1021/bi0019803

Pinto SN, Silva LC, de Almeida RFM, Prieto M (2008) Membrane domain formation, interdigitation, and morphological alterations induced by the very long chain asymmetric C24:1 ceramide. Biophys J 95:2867–2879. doi:10.1529/biophysj.108.129858

Pinto SN, Silva LC, Futerman AH, Prieto M (2011) Effect of ceramide structure on membrane biophysical properties: the role of acyl chain length and unsaturation. Biochim Biophys Acta Biomembr 1808:2753–2760. doi:10.1016/j.bbamem.2011.07.023

Regen SL (2002) Lipid–lipid recognition in fluid bilayers: solving the cholesterol mystery. Curr Opin Chem Biol 6:729–735. doi:10.1016/S1367-5931(02)00398-8

Risbo J, Sperotto MM, Mouritsen OG (1995) Theory of phase equilibria and critical mixing points in binary lipid bilayers. J Chem Phys 103:3643–3656. doi:10.1063/1.470041

Rosetti CM, Oliveira RG, Maggio B (2005) The Folch–Lees proteolipid induces phase coexistence and transverse reorganization of lateral domains in myelin monolayers. Biochim Biophys Acta Biomembr 1668:75–86. doi:10.1016/j.bbamem.2004.11.009

Rosetti CM, Oliveira RG, Maggio B (2003) Reflectance and topography of glycosphingolipid monolayers at the air–water interface. Langmuir 19:377–384. doi:10.1021/la026370d

Ruiz-Argüello MB, Basáñez G, Goñi FM, Alonso A (1996) Different effects of enzyme-generated ceramides and diacylglycerols in phospholipid membrane fusion and leakage. J Biol Chem 271:26616–26621. doi:10.1074/jbc.271.43.26616

Silva LC, de Almeida RFM, Castro BM, Fedorov A, Prieto M (2007) Ceramide-domain formation and collapse in lipid rafts: membrane reorganization by an apoptotic lipid. Biophys J 92:502–516. doi:10.1529/biophysj.106.091876

Silva LC, Futerman AH, Prieto M (2009) Lipid raft composition modulates sphingomyelinase activity and ceramide-induced membrane physical alterations. Biophys J 96:3210–3222. doi:10.1016/j.bpj.2008.12.3923

Siskind LJ, Colombini M (2000) The lipids C2- and C16-ceramide form large stable channels: implications for apoptosis. J Biol Chem 275:38640–38644. doi:10.1074/jbc.C000587200

Sot J, Aranda FJ, Collado M-I, Goñi FM, Alonso A (2005) Different effects of long- and short-chain ceramides on the gel-fluid and lamellar-hexagonal transitions of phospholipids: a calorimetric, NMR, and x-ray diffraction study. Biophys J 88:3368–3380. doi:10.1529/biophysj.104.057851

Sot J, Bagatolli LA, Goñi FM, Alonso A (2006) Detergent-resistant, ceramide-enriched domains in sphingomyelin/ceramide bilayers. Biophys J 90:903–914. doi:10.1529/biophysj.105.067710

Sot J, Collado MI, Arrondo JLR, Alonso A, Goñi FM (2002) Triton X-100-resistant bilayers: effect of lipid composition and relevance to the raft phenomenon. Langmuir 18:2828–2835. doi:10.1021/la011381c

Staneva G, Chachaty C, Wolf C, Koumanov K, Quinn PJ (2008) The role of sphingomyelin in regulating phase coexistence in complex lipid model membranes: competition between ceramide and cholesterol. Biochim Biophys Acta Biomembr 1778:2727–2739. doi:10.1016/j.bbamem.2008.07.025

van Blitterswijk WJ, van der Luit AH, Veldman RJ, Verheij M, Borst J (2003) Ceramide: second messenger or modulator of membrane structure and dynamics? Biochem J 369:199–211. doi:10.1042/BJ20021528

Vega Mercado F, Maggio B, Wilke N (2012) Modulation of the domain topography of biphasic monolayers of stearic acid and dimyristoyl phosphatidylcholine. Chem Phys Lipids 165:232–237. doi:10.1016/j.chemphyslip.2012.01.003

Veiga MP, Arrondo JL, Goñi FM, Alonso A (1999) Ceramides in phospholipid membranes: effects on bilayer stability and transition to nonlamellar phases. Biophys J 76:342–350. doi:10.1016/S0006-3495(99)77201-2

Veiga MP, Goñi FM, Alonso A, Marsh D (2000) Mixed membranes of sphingolipids and glycerolipids as studied by spin-label ESR spectroscopy. A search for domain formation. Biochemistry 39:9876–9883. doi:10.1021/bi000678r

Westerlund B, Grandell PM, Isaksson YJE, Slotte JP (2010) Ceramide acyl chain length markedly influences miscibility with palmitoyl sphingomyelin in bilayer membranes. Eur Biophys J 39:1117–1128. doi:10.1007/s00249-009-0562-6

Wilke N, Maggio B (2009) The influence of domain crowding on the lateral diffusion of ceramide-enriched domains in a sphingomyelin monolayer. J Phys Chem B 113:12844–12851. doi:10.1021/jp904378y

Wilke N, Vega Mercado F, Maggio B (2010) Rheological properties of a two phase lipid monolayer at the air/water interface: effect of the composition of the mixture. Langmuir 26:11050–11059. doi:10.1021/la100552j

Yu RK, Bieberich E, Xia T, Zeng G (2004) Regulation of ganglioside biosynthesis in the nervous system. J Lipid Res 45:783–793. doi:10.1194/jlr.R300020-JLR200